High-pressure infrared study of solid methane: Phase diagram up to 30 GPa

Roberto Bini* and Gabriele Pratesi†
European Laboratory for Nonlinear Spectroscopy (LENS), Largo E. Fermi 2, 50124 Firenze, Italy
(Received 28 October 1996)

High-pressure infrared spectra of solid methane are reported up to 30 GPa between 50 and 300 K. The symmetric stretching mode (ν_1) was successfully used as a probe of the phase transitions. Seven different phases have been identified. Pressure and temperature-dependent studies allowed us to outline all the phase boundaries in this portion of the diagram. A high-pressure phase (HP), stable in all the temperature range analyzed, has been identified. The transition to this phase occurs at about 8 GPa at 50 K, and 25 GPa at 300 K. The wide range of stability of this phase suggests a single site-ordered structure. Group-theoretical and qualitative arguments point to hcp (D_{6h} factor group) as the favored crystal structure of the HP phase. The knowledge of the phase diagram allows us to outline the evolution of the crystal structure and of the site symmetries as the pressure increases. The low-pressure fcc crystalline modifications transform to the fully ordered hcp structure through intermediate tetragonal phases. Competition between molecular and crystalline fields determines a complex site-symmetry evolution. Similarities with analogous fcc-hcp evolution observed in rare gases and atomic systems support our conclusions. [S0163-1829(97)00122-7]

INTRODUCTION

The increasing availability of spectroscopic data concerning the icy surfaces of planets and satellites of the solar system originated in the last few years a renewed interest in molecular crystals. Several molecules in condensed phase, including methane, and binary mixtures, such as N_2:CH_4, have been identified.[1,2] The spectral properties of these ices are the subject of a recent review.[3] It appears important, when discussing the astrophysical implications of these data, to have a detailed knowledge of the phase diagram of the solids of interest. However, while temperature or pressure-dependent studies are frequently reported, the simultaneous variation of P and T is by no means a trivial task to pursue. On the other hand, well-defined phase diagrams of pure solids are a prerequisite to understand the thermodynamic stability of binary mixtures commonly found on planets or prepared in laboratory experiments. Quite recently it has been found that methane forms solid compounds with hydrogen under pressure.[4] The effect of pressure on the chemical interactions in this class of compounds are important from the chemical, geophysical, and technological point of view.

In this paper attention is focused on the phase diagram and the phase transitions of pure CH_4 crystal. Despite the large amount of vibrational data as a function of temperature and/or pressure, only the low-pressure portion ($P \leqslant 0.5$ GPa) of the diagram is well characterized.[5–16] Besides the fcc structure of plastic phase I,[5] to which liquid methane crystallizes between 100 and 300 K, only that of phase II, stable below 25 K, is known. The space group is $Fm3c$ (fcc) with eight molecules per unit cell, six orientationally ordered on D_{2d} sites while the other two, on O sites, behave as weakly hindered rotators.[5] As to phase III, occurring in a limited pressure range at low temperature, a three-site occupancy is suggested by several Raman and infrared results, however without a definite indication on the symmetry of these sites which are commonly denoted as S_1, S_2, and W.[6] Molecules lying on the first two sites experience strong rotational fields while those on W have a relatively high degree of rotational freedom. Raman experiments at 4 K up to 1.1 GPa suggest the occurrence of other three phases, in addition to III.[6,13,15] Evidence of two of them (IV and V) comes from slope changes in the frequency vs pressure plot of the lattice phonons and ν_3 side bands, while most other spectral features are similar to those of phase III. Phase VI is observed for pressures larger than 1 GPa, considering the spectral changes in the ν_1 band.

At room temperature, Raman, Brillouin, and refractive index measurements provide evidence of a transition at 5 GPa from I to a different phase, hereafter indicated as phase A, reportedly correlated to the low-temperature phase IV and with a disordered hcp structure.[17] A second crsytalline change is observed during compression around 12 GPa. This phase transition exhibits a considerable hysteresis given that the higher pressure modification, hereafter indicated as phase B, is stable down to 6 GPa during expansion. Recent infrared data on the symmetric (ν_1) and antisymmetric (ν_3) stretching modes confirmed the two transitions and allowed to locate more precisely (between 7.5 and 9 GPa) the A-B transformation by careful kinetics studies.[18] Structural inferences on these phases were proposed from a combined analysis of the infrared and Raman data.[18] As to phase A, a correlation with the low-temperature multisite structures was attempted. The observed three ν_1 components (two Raman and one infrared) do not agree with the proposed hcp disordered structure.[17] As to phase B, a single-site occupancy with C_s symmetry was assumed with unit-cell symmetries restricted to D_{4h}, D_{6h}, T_d, and O_h factor groups. Qualitative considerations on crystal packing of CH_4 molecules and similarities with the behavior of the homologous, more anisotropic, NH_3 crystal favor the D_{6h} hcp as the most plausible structure. These results give importance to infrared and Raman data for structural analyses when a direct investigation, through x-ray diffraction or elastic neutron-scattering studies, is not available.

A question left open by these studies is the correlation

between low- and room-temperature results, due to the lack of information on the crystal CH_4 structures in a wide portion of the phase diagram in the intermediate range of temperature. As a part of a research project on solid-solid phase transitions in simple molecular crystals under high pressure, we report on the infrared spectrum of solid methane from 300 down to 50 K and at pressures up to 30 GPa. To this purpose it was experimentally necessary to couple our high-pressure infrared apparatus to a cryogenic system. The band profile of the ν_1 mode was used as a probe of the phase transitions, as already successfully done in room-temperature experiments.[18] The experimental observations are discussed on the basis of the current structural information on solid methane. The phase diagram of CH_4 crystal has been determined in detail above 50 K and a high-pressure phase (HP), stable in all the temperature range examined, discovered. This is, in our view, the fully ordered single-site crystal structure of solid methane.

EXPERIMENT

High-pressure infrared spectra of solid methane were measured using a membrane diamond-anvil cell (MDAC) equipped with IIa diamonds and a stainless-steel gasket. The cell was filled with CH_4 (99.99% purity) by means of high-pressure gas-loading equipment. Care was taken to purge the system several times before loading with a few hundred bars of methane. Once the loading was completed the pressure inside the cell was typically between 2 and 4 GPa, while the samples had thicknesses ranging from 50 to 80 μm and diameters from 150 to 250 μm. Ruby chips of about 10 μm were present in the sample for *in situ* pressure calibration.

The optical beam condensing system, the method to measure the ruby fluorescence as well as the equipment set to perform low-temperature infrared spectra at high pressure have been extensively described elsewhere.[18,19] Briefly, the MDAC is mounted on a copper holder attached to the cold tip of a close-cycle cryostat (APD model DE 204-SL). Thermal contact is ensured by thin indium foils. The cryostat moves on orthogonal tables and is connected via a shock absorbing bellow to the sample compartment of a Fourier transform infrared (FTIR) spectrometer (IFS 120 HR-Bruker). The latter is separated from the rest of the instrument by means of CsI windows, which ensure the transmission of the infrared light as well as the laser beam and the ruby fluorescence emission, and is evacuated to $10^{-4}-10^{-5}$ bars in order to lower the sample temperature. The infrared beam is focused onto the MDAC, whose fine adjustment is achieved through micrometric translation stages, and afterward collected by Cassegrain-type objectives. The pressure in the MDAC can be continuously varied from outside of the spectrometer by regulating the helium pressure in the membrane through a capillary pipe entering the instrument compartment. The sample temperature is monitored with a thermocouple soldered onto the gasket. A periscope, located just outside the sample compartment, can be inserted on the infrared beam path allowing the visual observation of the sample with a microscope. The same optical path is used also to excite the ruby chip with 10–20 mW of the 514.5 nm line of an Ar^+ laser and to collect backward the ruby fluorescence measured with a dedicated spectrometer. The pressure is determined from the peak wavelength of the R_1 ruby fluorescence band by using the equation:[20]

$$P(\mathrm{GPa}) = 380.8[(\lambda/\lambda_0)^5 - 1],$$

where the temperature-dependent peak wavelength at zero pressure λ_0 was measured according to the selected temperature for high-pressure experiments.

The FTIR spectrometer was equipped with a halogen lamp, a KBr beam splitter and a liquid-nitrogen-cooled MCT detector. The spectral resolution was 0.9 cm^{-1} in all the measurements.

RESULTS

The CH_4 molecule has four internal vibrational modes (A_1+E+2F_2) all of which exhibit Raman activity, while only the two triply degenerate F_2 modes (ν_3 and ν_4) are infrared active. We focus our attention on the symmetric stretching mode (ν_1) whose infrared activity in the solid is entirely due to crystal-field effects. Accordingly the absorption in the ν_1 region is an accurate probe of the phase transitions, as already observed in room-temperature studies.[18] Furthermore, the number of ν_1 infrared components being directly related to factor group and site symmetries, the infrared spectrum in the symmetric stretching region provides indications about the structural properties of the methane crystal. A similar study on the close-lying absorption band of the antisymmetric stretching mode (ν_3) was not equally informative, due to the intrinsic strength of the ν_3 mode in the isolated molecule and its large enhancement as the temperature is lowered. As a matter of fact, only in a few experiments in the high-pressure range ($P \geqslant 13$ GPa) was the ν_3 absorption sufficiently weak to be analyzed with accuracy also at low temperatures.

We report here the results of several experiments carried out on different samples. A standard procedure was used in most experiments. Once phase *B* was produced at room temperature and pressures between 12 and 14 GPa,[18] the sample was cooled either at constant or variable pressure. The evolution with pressure of the ν_1 infrared absorption was studied at different temperatures so that the phase boundaries were determined at constant pressure and at constant temperature. A few experiments were performed cooling room-temperature phases I, *A*, and HP.

The pressure at which a phase transition occurs at constant temperature is usually estimated following the pressure dependence of the vibrational frequencies. Alternatively, bandwidths (Γ) and integrated band intensities (A) have been measured as a function of pressure in this work. While in the first case the transition pressure is determined by the slope change in the ν vs P plot, an abrupt variation of Γ and A is observed in the other two plots, from which an even more accurate value of the transition pressure is found. Constant temperature experiments show that when a transition is completed a general decrease in the Γ values is found increasing pressure. The change in the Γ and, more indirectly, A parameters must be related to the following phenomena. First, an inhomogeneous broadening due to the disorder induced by structural changes is expected when the phase transition is approached; second, the crystal potential being close

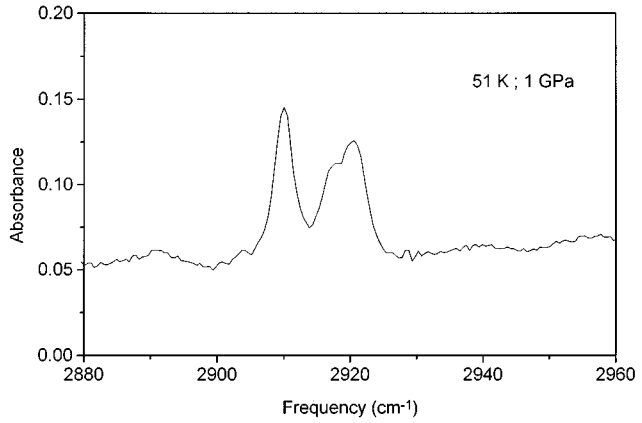

FIG. 1. Infrared spectrum of the ν_1 mode of solid methane at 51 K and 1.0 GPa.

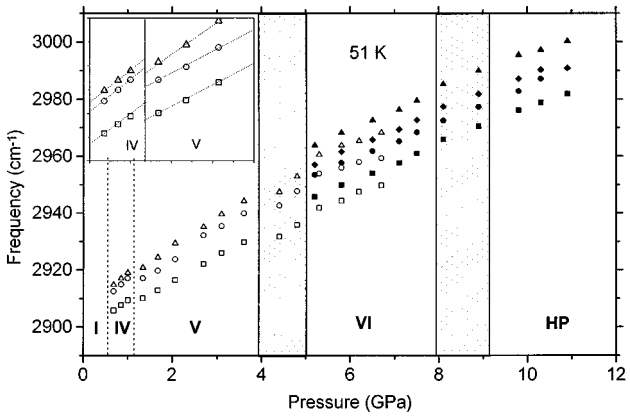

FIG. 2. Pressure dependence of the frequency of the ν_1 infrared components at 50 K. Empty symbols correspond to measurements collected pressurizing phase I samples. Full symbols are related to experiments performed on samples cooled to 50 K through a quasi-isobaric path. Dashed regions indicate the pressure range where the transition are located. The inset shows in detail the region of the IV-V transition.

to the transition strongly anharmonic, the usual picture, which explains the vibrational relaxation mainly in terms of processes involving few crystal phonons (cubic and quartic),[21,22] is not applicable anymore because higher-order mechanisms will open new decay channels. Integrated band intensities depend also on the sample thickness, which is not constant during compression. However, data obtained in small pressure ranges, or during expansion, are reliable to locate phase transitions and to correlate the Davydov components of adjacent crystal modifications.

The results concerning the different phases are presented in different subsections for the sake of clarity. The room-temperature crystal phases will be labeled as I, *A*, and *B* as in Ref. 18, while those occurring at low temperature according to the notation of Ref. 15. Complementing with data at intermediate temperatures, a correlation between the two portions of the phase diagram may be proposed.

Phase I

This fcc plastic phase, containing one molecule per cell, does not exhibit ν_1 infrared activity. Therefore solid-solid equilibrium curves for this phase may be easily obtained in the phase diagram. Constant temperature measurements (100, 136, 150, 208, and 298 K) allowed us to identify, from the appearance of a single band increasing pressure or from its disappearance releasing it, the boundary with phase *A*. The I→*A* transformation is also induced cooling the sample at constant pressure at 125 and 250 K. At 51 K the transition from phase I to a crystal modification different from phase *A* is observed between 0.5 and 0.7 GPa. This is suggested by the appearance of a triplet structure for ν_1 instead of the singlet associated with phase *A*. More details about this transition will be given in the subsection concerning phase IV.

Phase *A*

At room temperature one weak infrared and two Raman bands have been observed for this phase.[18] As already stated in the previous section the I-*A* phase boundary is quite well defined. It is more difficult to establish the *A*-*B* phase boundary. At room temperature, the *A*-*B* transition is sluggish and affected by hysteresis either during expansion or compression.[17,18] In constant temperature experiments performed at 108, 136, and 165 K, the ν_1 doublet, typical of phase *B*, disappears releasing the pressure being substituted by the weak singlet of phase *A*. On the contrary, phase *B* is never induced from phase *A*, below room temperature, with increasing pressure. This is in close agreement with room-temperature kinetics data showing a freezing of the *A* structure once the pressure is increased without a time stop of several hours.[18] The stability range of phase *A* does not extend below 80 K given that no singlet ν_1 band is observed during expansion at temperatures lower than this value.

Phase *B*

At room temperature the ν_1 infrared mode is split into a doublet in the *B* phase.[18] Both components have bandwidths sensibly reduced to about 4 cm^{-1} lowering the temperature (108 K; 2.1 GPa) from the room-temperature value of 11–12 cm^{-1} at 9 GPa. Shoulders or asymmetries, which could indicate the occurrence of additional components hidden at higher temperature by line broadening, are never observed. Releasing pressure the *B* doublet always transforms in the *A* singlet. Below about 100 K however, a triplet band structure is obtained independently of the sample and the cooling path. On the other hand, increasing the pressure a transition to a different phase (in the following denoted HP) is observed. The discussion on the *B*-HP phase transition and the HP spectrum will be postponed, following the subsections on the low-temperature crystal phases.

Phase IV

At 4.2 K phase IV has a stability range between about 0.2 and 0.5 GPa as it results from the slope changes plotting the librational energies associated with S_1, S_2, and *W* sites as a function of pressure. This was confirmed by the evolution with pressure of the Raman phonon frequencies.[13] The transition from the disordered phase I to phase IV was also studied below 90 K and 0.9 GPa by NMR spectroscopy.[16] From our infrared spectrum the transition is observed between 50 and 70 K at pressure values ranging from 0.6 to 0.8 GPa, in

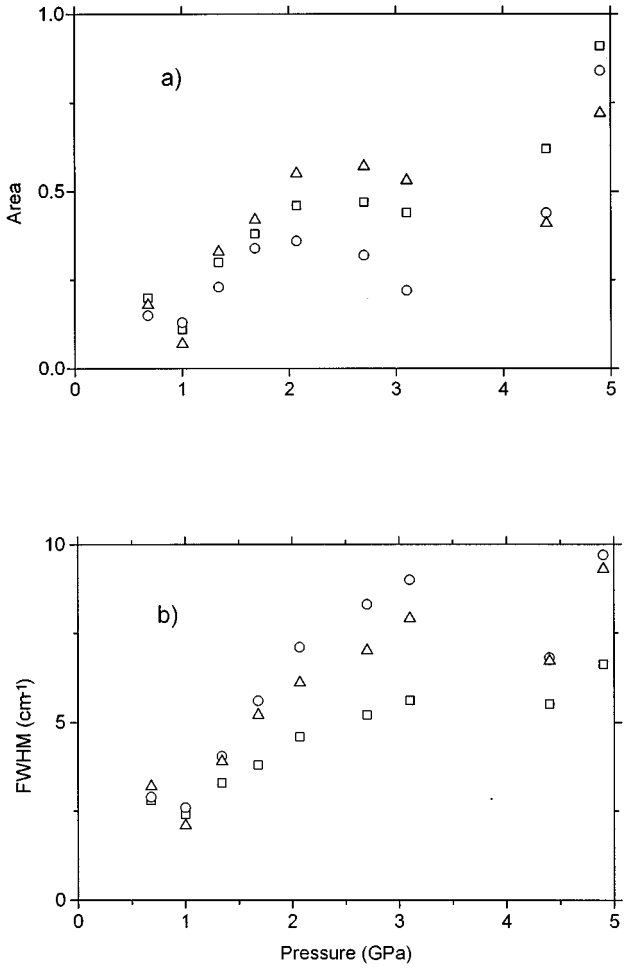

FIG. 3. Area (absorbance units)(a) and fullwidth (b) dependence on pressure of the three ν_1 infrared components of solid methane at 50 K. Components are indicated with the same symbols of Fig. 2.

good agreement with the NMR study. The absorption of the symmetric stretching region is split into a triplet. The central component is weak and occurs as a shoulder of the high-frequency peak (Fig. 1). At 51 K the stability range of phase IV, $\approx$0.3 GPa as at 4.2 K, shifts to higher pressures. Considering Fig. 2, where the frequency values collected at 51 K as a function of pressure are reported, the transition to a different phase (V) may be located at about 1.2 GPa. Correspondingly the abrupt change of linewidths and integrated absorptions for the three components around 1 GPa is shown in Fig. 3. The formation of phase IV has been always observed between 48 and 66 K independently of the sample quality, either during compression (I→IV) or expansion (V→IV) experiments.

Phases V and VI

The portion of the phase diagram below 100 K and between 1 and 9 GPa has been probed in ten different experiments. The structure of the ν_1 multiplet slightly changes depending on the sample history, i.e., on the temperature/pressure path followed in each experiment. As an example, we report in Fig. 4 two spectra at 50 K and 6.5 GPa. The upper trace shows the spectrum usually obtained when the sample is pressurized from phase IV. The well resolved multiplet observable in the lower trace, is due to a different sample preparation according to the following procedure. First the $A \rightarrow B$ phase transition was induced at room temperature and relatively low pressure (11 GPa) and the B crystals cooled adding some helium gas in the membrane so that the pressure inside the cell decreased down to $\approx$5 GPa at about 125 K. Then the sample was isobarically cooled to 50 K. Looking at Fig. 4 it is concluded that the latter procedure gives crystals of higher quality, even though the sample undergoes a greater compression. On the whole, the two spectra are quite similar apart from a small relative frequency shift and larger linewidths in the upper trace with a consequent loss of spectral resolution. In Fig. 2 the frequencies of the observed ν_1 components, measured on samples prepared with both procedures and fitting the upper type spectra with only three bands, are reported as a function of pressure. The empty symbols, collected either increasing or releasing pressure, correspond to data obtained on samples which have been pressurized from phase IV. The full symbols are related to samples cooled at 50 K following the second procedure (quasi-isobaric cooling). Same symbols are employed to identify, whenever possible, the corresponding bands in the two cases. Beside the IV-V phase transition, another phase

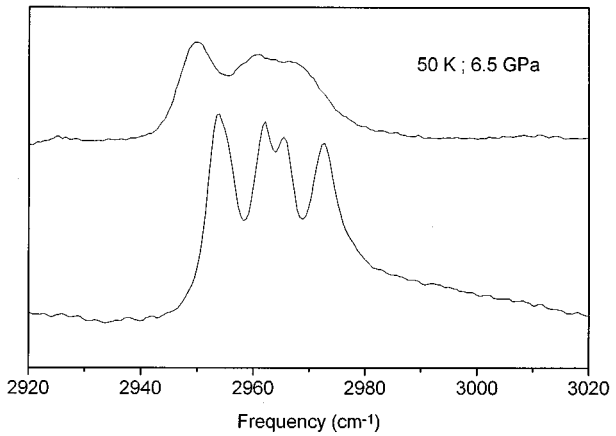

FIG. 4. ν_1 spectra collected at 50 K and 6.5 GPa. Upper trace: sample produced pressurizing phase I; lower trace: sample cooled to 50 K through a quasi-isobaric path.

TABLE I. Pressure coefficients, $d\nu/dP$ (cm^{-1}/GPa), of the symmetric stretching infrared components in the different phases obtained in isothermal expansion and compression experiments.

T (K)	IV	V	VI	B	HP
	11.25	8.86	6.75		5.27
51	14.06	10.51	6.41		
			6.81		
	13.13	10.36	7.12		4.39
		4.87			7.09
117		5.15			
		7.12			9.05
300				5.15	10.60
				5.66	8.98

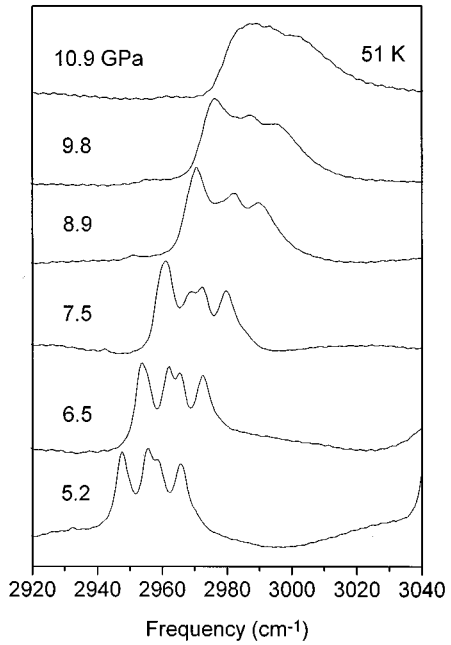

FIG. 5. Evolution of the ν_1 absorption between 5 and 11 GPa at 50 K.

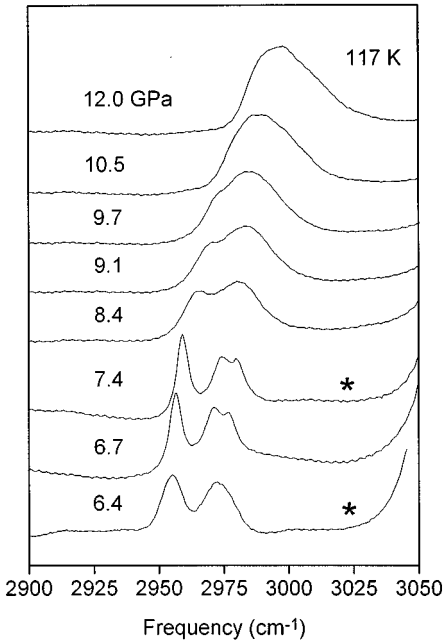

FIG. 6. Evolution of the ν_1 infrared spectrum at 117 K releasing pressure between 6.7 and 12 GPa. The two spectra labeled with an asterisk have been obtained in a different experiment increasing pressure.

change occurs around 4 GPa. A slope change is found in the dependence on pressure of the frequencies of the three components (see Fig. 2). Further, in Fig. 3(a) a significant reduction of the integrated absorption of the high-frequency component is observed between 3 and 4 GPa, while that of the central component increases by a factor of 2. Finally, a phase change is suggested also from the behavior of the linewidths in the same pressure range as reported in Fig. 3(b). When the pressure is larger than 5 GPa the mode frequencies soften appreciably with pressure. Slopes in this region are smaller than between 1 and 4 GPa (see Table I).

In Fig. 5 the evolution with pressure of the ν_1 multiplet, for samples prepared with the quasi-isobaric cooling, is shown. A change in the relative intensities of the central components is observed when the pressure is increased. Around 9 GPa a reduction in the number of ν_1 components and a merging takes place. The analysis of Γ, A, and ν values, discussed in detail in the next paragraph, indicates that a transition to a higher-pressure phase occurs.

Infrared ν_1 multiplets closely recalling those of phase V were observed below 8–9 GPa up to 100 K on samples cooled from phase *B* or produced after expansion from the HP phase. Despite these spectra having been measured at higher pressures and temperatures, with respect to those pressurizing phase IV, a higher quality is noticed. As an example, Fig. 6 shows (spectra labeled by an asterisk) the sudden transformation of the phase *B* doublet into the triplet of phase V during an isothermal compression experiment at 117 K between 6.4 and 7.4 GPa. In the same figure are also presented the rapid spectral changes which occur releasing pressure from 12 to 6.7 GPa. In Fig. 7 the corresponding frequencies vs pressure are plotted.

The high-pressure phase

A high-pressure phase (HP), whose infrared absorption in the ν_1 region is characterized by two not-well-resolved peaks giving rise to a broad, strongly asymmetric band, may be isolated from room temperature, over 25 GPa, down to 50 K and 9–10 GPa. The doublet separation changes from 13 cm^{-1} at 50 K up to 25 cm^{-1} at room temperature without affecting the general survey of the spectrum. The high-frequency component is broader and its absorbance is generally greater by a factor of 1.5–2 of the low-frequency band. The transition to the HP phase is easily induced independently of the temperature and no appreciable hysteresis was recorded in the obtainment of lower-pressure crystal structures. The transition to the HP phase, either from *B* or low-temperature phases (and vice versa), has been studied at several temperatures cooling at constant pressure. Isothermal reversible studies of the transitions have been also performed at 51, 100, 108, 117, 136, 165, 208, and 300 K. The results at 117 K are presented in Figs. 6 and 7. The integrated absorp-

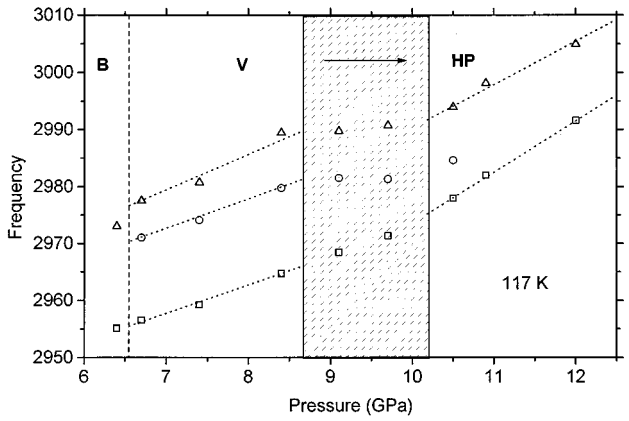

FIG. 7. Pressure evolution of the peak frequencies relative to the experiments performed at 117 K and shown in Fig. 6. Dashed regions indicate the pressure range where the transition is located.

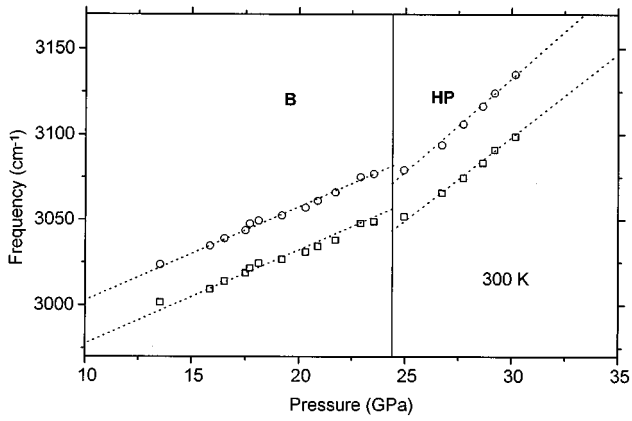

FIG. 8. Frequency variation with pressure of the ν_1 components at 300 K up to 30 GPa.

tion of the ν_1 band is almost constant up to 9 GPa. Between 9 and 12 GPa, the intensities of the lower and upper components increase by a factor 2.5–3, while the central component almost disappears at 10.5 GPa. The latter point was carefully checked also considering frequency and width data of the three components. In Fig. 8 the frequency dependence on pressure at room temperature of the two ν_1 components are reported. An evident slope change takes place at 25 GPa but a doublet still characterizes the high-pressure spectra. Even more difficult is the discussion of the transition to the HP phase studied at 51 K. In fact, as can be seen from Fig. 2, there is not a clear discontinuity in the frequency values above 5 GPa even though the slope values, reported in Table I, remark a softening of the frequencies dependence on pressure above 9 GPa. Also in this case the frequency vs pressure plot is the result of a data analysis involving cross checks with linewidths and integrated areas. In Fig. 9 the resulting absorption values of the four components are reported. In this figure an inset shows in detail the evolution of the corresponding frequencies in the same pressure range. Up to 7 GPa the absorbance values are quite constant then a sudden increase of the high-frequency component is observed. Also the low-frequency band has a similar behavior but is not so

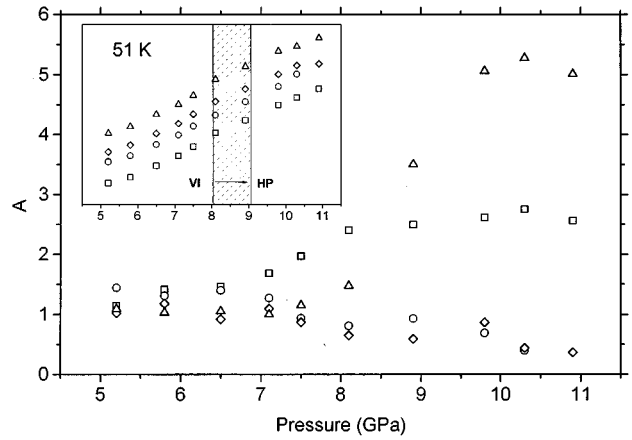

FIG. 9. Integrated absorption dependence on pressure of the ν_1 infrared components at 50 K between 5 and 11 GPa. In the inset the variation of the frequencies is reported. Same components are indicated with the same symbols.

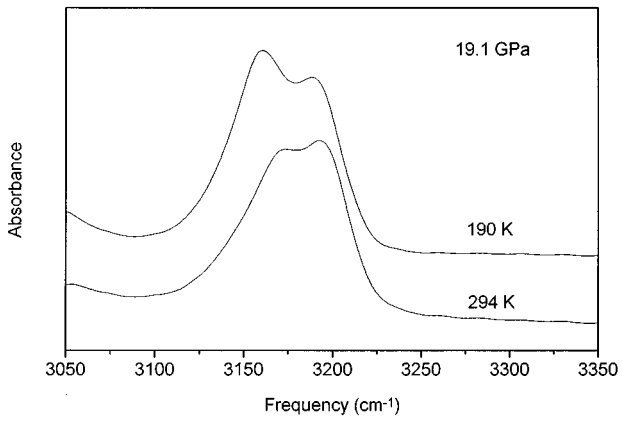

FIG. 10. Profile of the ν_3 mode in the B (lower trace) and HP (upper trace) phases as obtained in an isobaric cooling experiment at 19.1 GPa.

pronounced, in fact at 7 GPa its area is about 2 times that of the high-frequency band, while at 10 GPa this ratio is exactly reversed. The area of the central bands start to decrease at 7 GPa and comes progressively closer to zero as the pressure increases. Above 10.5 GPa only one band is necessary, in the central region of the multiplet, to reproduce the observed ν_1 profile nevertheless the central absorption still decreases. Finally, around 11.5 GPa a doublet fits perfectly the experimental absorption. These results attest a structural transformation which starts around 7 GPa and is completed between 10 and 11 GPa.

It is worth also noticing that for this phase we succeeded in having some low-temperature high-pressure spectra of the ν_3 components without the complete saturation of the absorption. In Fig. 10 the ν_3 absorption is shown before and after the $B \rightarrow$HP transition during an isobaric cooling at about 19 GPa. A change in the intensity distribution of the different components takes place but, as observed in the ν_1 structure, there is no evidence of a different number of peaks.

The phase diagram

In the previous paragraphs we have shown the spectral behavior of the ν_1 absorption in different regions of the P-T diagram. According to these results a direct identification of the phase boundaries can be sketched, taking advantage also of the spectroscopic data obtained at low[6–8,13–16] and room temperature.[17,18] In Fig. 11 the phase diagram of solid methane between 0 and 300 K and below 30 GPa is presented. The points reported in the diagram represent the regions probed during the different experiments. As to phases I and HP, only data near the boundaries are shown. For phase I, measurements down to 0.1 GPa have been performed, while for the HP phase measurements up to 30 GPa at room temperature, and to 18 GPa at 50 K have been performed. Same symbols are used to indicate similar spectra. Solid-solid equilibrium curves have been drawn according to the spectral profile in the ν_1 region and the accurate analysis of frequency, integrated absorption, and linewidth data as a function of pressure. When different symbols are present in a region it means that the phase transition is affected by hysteresis, with particular reference to the A-B transition. Only in the dashed region around 75 K and 1 GPa was it difficult

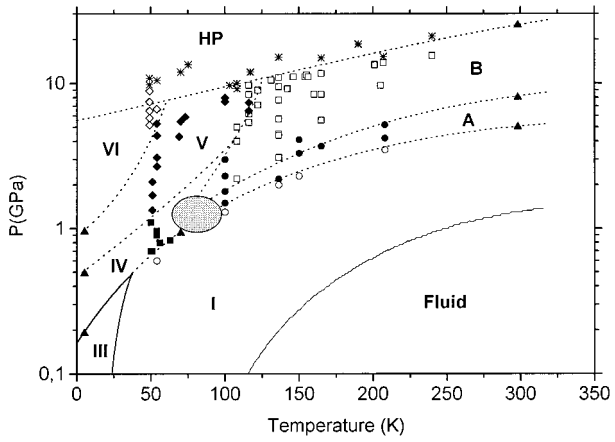

FIG. 11. Phase diagram of solid methane as it results from the present experiments. Solid lines indicate the phase boundaries already characterized (Ref. 4). Dashed lines are the phase boundaries extracted from the present study and from the data (full triangles) at 4, 80, and 300 K (Refs. 5, 12, 14, 15, 24, and 25). Same symbols indicate same spectral features of the ν_1 absorptions and have been assigned as: empty circles phase I, full circles phase *A*, empty squares phase *B*, full squares phase IV, full rhombs phase V, empty rhombs phase VI, stars phase HP. The dashed area represent a region where the results do not allow an accurate determination of the boundaries of the different phases.

to locate the boundaries of the four phases present in this part of the diagram.

DISCUSSION

From the present information on the phase diagram and from previous studies, at low and room temperature, structural inferences on solid methane may be advanced. The room-temperature *A* phase extends from 300 down to about 80 K. Below this temperature down to 0 K, and at pressures larger than those of the well characterized I, II, and III phases, a different crystal modification (IV) is stable. The latter phase presents the following similarities with phase *A*: (a) the transition from the disordered phase I takes place easily in the 50–80 K temperature range; (b) no appreciable hysteresis is noticed when the pressure is released going back to phase I. These observations point to similar crystal structures of the I, IV, and *A* phases.

As far as phase IV is concerned, a tetragonal crystal structure consisting of three different types of site is generally assumed.[7,8,12,23] This model was adopted by Fabre and co-workers[6,13,15] in the interpretation of their Raman results without indication of site symmetry. As to the factor-group symmetry, the D_{4h} was preferred to D_{2d} symmetry due to the lack of coincidence among infrared and Raman frequencies of the lattice modes.[8] The D_{4h} factor group symmetry is supported also by the present results: at 50 K and 0.8 GPa the ν_1 infrared components fall between 2907.5 and 2917.0 cm^{-1}. We can compare this observation with Raman results at 4.2 K,[6,13,15] where two peaks are seen, for pressure values from 0.01 to 0.86 GPa, with an almost constant frequency separation not exceeding 6 cm^{-1}. The anharmonic and volume contributions to the frequency shift, as reported for several other molecular crystals, cannot account for a frequency dispersion doubling between 4 and 50 K. Therefore also in the ν_1 case there is not a coincidence of infrared and Raman peaks, as expected for D_{4h} crystal symmetry. On the contrary, for the D_{2d} factor-group symmetry all the components should have infrared and Raman activity. A preliminary selection of the site symmetries can be attempted on the basis of three different ν_1 components. For a crystal composed by tetrahedral molecules (T_d) and having a D_{4h} factor-group symmetry, the common subgroups, which give the symmetry of the possible sites, are D_{2d}, S_4, D_2, C_{2v}, C_2, C_s. Among these, only the C_{2v}, C_2, and C_s give infrared activity originating 1, 1, and 2 components, respectively. Therefore, beside the C_s site, which must necessarily be present in order to have three different peaks, one between the C_{2v} and C_2, and another one among D_{2d}, S_4, and D_2, sites must be chosen.

In the *A* phase the observation of a single infrared band and two Raman peaks,[18] having different frequencies, does not allow us to speculate about the structure. We have already found that the I-*A* transition takes place reversibly, consisting only in a moderate hindering of the free rotation of CH_4 molecules with consequent formation of lower symmetry sites, which induce the splitting of the Raman band and the weak infrared activity. On the contrary the *A*-*B* transition has been observed at room temperature to be extremely slow in compression and undergoes a large hysteresis during expansion.[18] In the present experiment, where no kinetics studies have been performed, the $A \rightarrow B$ transition has been never observed, between 100 and 210 K, confirming that a complex structural rearrangement takes place between the *A* and *B* phases.

In the previous room-temperature study,[18] an analysis of the *B* phase was carried out applying group-theoretical arguments to infrared and Raman results. Assuming a single-site structure, the unit-cell symmetries in agreement with experiment were D_{4h}, D_{6h}, T_h, O_h; all with a C_s site symmetry. Kinetic data on the $A \rightarrow B$ transition contrast with transition to a tetragonal (D_{4h}) or cubic (T_h,O_h) *B* structure, being likely a similar structure for phase *A*, and suggest the hexagonal D_{6h} as the most probable factor group. The results presented in this work allow a deeper insight about the structure of phase *B*. The *B*-HP transition, between 125 and 300 K, occurs rapidly either in compression or expansion experiments. The number of ν_1 and ν_3 components are conserved and the *B* and HP multiplets look quite similar. This may be a reasonable indication that the two phases have similar structures and that only a site change, or a reduction in the number of sites, takes place. Our hypothesis agrees with early results from Brillouin scattering.[17] The dispersion of the Brillouin-frequency shift between 12 and 25 GPa is consistent with the $A \rightarrow B$ transition starting at 12 GPa and terminating only at 25 GPa. Above 25 GPa the definitive formation of phase *B* is claimed due to the lack of dispersion of the Brillouin frequency shift. However, we clearly showed that phase *B* is, according to our results, a well-defined crystal modification stable in a large range of temperature and pressure. Therefore, the observed behavior of the Brillouin shift can be explained assuming more than one site for phase *B* and only one for the HP phase. The wide pressure and temperature range of the HP stability supports an ordered single-site structure. On this basis the past assumption of a

single-site structure for phase *B* must be reconsidered. Nevertheless if a multisite structure occurs in phase *B*, only a unit cell of high symmetry agrees with the high number of ν_1 components (at least three Raman and two infrared) observed in this phase. All this evidence indicates a common hexagonal close-packed structure for the *B* and HP phases but a different local molecular symmetry. The group-theoretical analysis, reported in Ref. 18, can be therefore extended to the HP phase. This interpretation implies a transformation from the fcc (I) to the hcp (*B*) structure involving the distortion of the original structure and the slip of alternate planes. Even though the rearrangement may be not favored kinetically, there are several experimental and theoretical cases of fcc-hcp transitions. Since the methane molecule may be approximately taken as spherical even at high pressure, a suitable comparison can be made with atomic and rare-gas solids. Molecular-dynamics calculations have been performed on Ni single crystals where the fcc structure evolves under uniaxial compression first to a tetragonal structure and then, on further compression, to an hcp structure under an highly coordinate transformation.[24] Experimentally the fcc-hcp transformation has been observed in solid Xe.[25] The low-pressure ($\leqslant$10 GPa) fcc structure transforms into hcp above 50 GPa going through a nonidentified intermediate modification. A similar fcc-hcp evolution was theoretically anticipated for compressed Ar on the basis of three-body anisotropic interactions.[26] In solid Kr the fcc structure may not be stable above 30 GPa according to x-ray-diffraction and Brillouin-scattering experiments.[27] On the other hand, the methane molecule can be thought as a ''bad'' rare gas, and therefore its greater anisotropy may help the fcc-hcp transition to occur at lower pressures. In the case of ammonia, which can be regarded as a pseudo CH_4 molecule with even stronger anisotropic interactions, such a fcc-hcp (III$\rightarrow$IV) transition was observed in an x-ray work around 4 GPa.[28] This result was not confirmed by recent neutron-diffraction studies on deuterated ammonia[29,30] showing that phase IV is orthorhombic, space group $P2_12_12_1$, and stable up to 12 GPa. It should be noted, however, that between 6 and 9 GPa the nitrogen positions move reducing the difference of the actual crystal packing from an ideal hcp arrangement. Furthermore, the stability of the hcp nitrogen arrangement up to 56 GPa (Ref. 28) supports the idea that the evolution with pressure of solid ammonia has common aspects with that observed at room temperature in solid methane (I-*A*-*B*-HP).

On this basis the discussion on the low-temperature portion of the phase diagram is easier to face. In the Results section we noted that the quality of the spectra collected in phase V was different depending on how the phase was obtained. Nicely resolved multiplets were observed coming from phases *B* and HP, while broad and unresolved band structures, even at lower pressure and temperature, when phase V was produced compressing phase IV. This may be explained considering that also at low temperatures a transformation from the fcc structure of phase I to the close-packed hexagonal HP phase occurs. The tetragonal structure of phase IV,[7,8,12,23] proposed on a completely different basis, matches perfectly the first step observed in the molecular-dynamics simulation of a Ni fcc-hcp transition,[24] corresponding to the distortion of the cubic lattice to a face-centered-tetragonal crystal structure. The hcp structure appears when alternate planes slip each with respect to the other. Our experimental results suggest that the final step occurs in phase V. Therefore, in the quasi-isobaric cooling from phase B to phase V, and then VI high-quality spectra are obtained due to the fact that only a site rearrangement takes place, these modifications having all hcp structures. On the contrary, a complex structural rearrangement underlies the transition to hexagonal phase V upon compression of the tetragonal phase IV.

A further inspection of the present data allows us to sketch a possible site evolution in the different crystalline structures. As it is shown in Fig. 2 (see the inset) the discontinuity in the pressure evolution of the frequencies of the three infrared components just above 1 GPa can be interpreted as due to different crystal fields in the two phase even if the spectral profile is not much affected. Also the spectra at higher temperatures and pressures, following the HP-V or B-V transitions, are better resolved but the triplet structure closely resembles that of phase IV. These results compare well with Raman measurements at 4 K for which the IV-V transformation did not determine appreciable spectral changes.[13] Our view is that, going through the IV-V phase transition, the tetragonal$\rightarrow$hexagonal step is not accompanied by a site reorientation. The molecular orientation in the crystal results from the competition between molecular and crystalline field.[15] For instance, in phase II the former is predominant.[31] As the pressure rises, the effect of the crystalline field increases. At 50 K and below 4 GPa the molecular field is still larger than the other so that the site symmetry is conserved even if a change in the crystal structure occurs. Around 4 GPa the crystalline field lowers the symmetry of the molecular orientation and consequently the site symmetry. On this basis also the increase of the number of components in the VI phase can be explained. The following scheme regarding the site evolution increasing pressure accounts for all the experimental results. For phase III different sets of sites have been proposed.[12,23,32] A three-site structure fits well with different experimental results.[6–9] Raman experiments[7] agree with the structure advanced by Maki, Kataoka, and Yamamoto[23] predicting for a D_{4h} factor group, D_2, S_4, and C_s sites. Assuming the same factor group also for phase IV and still valid a three-site model,[13,15] the correct number (3) of infrared components is consistent with preservation of the D_2 and the C_s sites and the change of the S_4 into a C_{2v} site. With this site multiplicity more than two Raman components are expected, therefore, the observed Raman doublet[6,13] implies a near degeneracy of the frequencies of the A_{1g} and B_{1g} components and the weakness of the third component, of B_{2g} symmetry, originating from the C_s site. In fact, as already emphasized at the beginning of the discussion paragraph, one of the three infrared components is due to the C_{2v} and the remaining two to the C_s sites. The IV$\rightarrow$V transformation does not affect the site symmetry even if the structure becomes hexagonal. As the pressure further increases there is a site-symmetry reduction, from D_2 to C_2, triggering the V-VI transition. This makes a fourth component appear in the ν_1 infrared spectrum. On further compression the crystalline field definitely dominates over the molecular leading to the HP single-site structure (C_s) (see Fig. 5). The lack of the ν_1 central components, shown in

TABLE II. Structures, factor groups, and sites symmetries of the phases discussed in this work.

Phase	Structure	Factor group	Site
III[a]	Tetragonal	D_{4h}	D_2, S_4, C_s
IV	Tetragonal	D_{4h}	D_2, C_{2v}, C_s
V	hcp	D_{6h}	D_2, C_{2v}, C_s
VI	hcp	D_{6h}	C_2, C_{2v}, C_s
B	hcp	D_{6h}	$(D_2), C_s$
HP	hcp	D_{6h}	C_s

[a]Reference 23.

Fig. 9, after the VI-HP phase transition was completed, is therefore related to the disappearance of the C_2 and C_{2v} sites or their conversion to C_s symmetry. On the contrary the absence of a discontinuity in the frequency values, as well as in the slope of the frequency vs pressure curve, of the high- and low-frequency components, is easily explained with the transition between two hcp structures preserving the same site symmetry, being these two bands likely induced by the C_s site. As far as phase *B* is concerned only D_2 sites are probably present, beside the C_s sites, and they contribute only to Raman activity. In this case, as already discussed for the VI-HP transition, no appreciable changes are expected and observed in the infrared spectra of the ν_1 mode going to the HP phase. In Table II a summary of the structures and of the site symmetry relative to the different phases discussed in the present work are presented.

CONCLUSIONS

In this paper we have reported on the ν_1 infrared spectrum of solid methane in a wide pressure range between 50 and 300 K. We demonstrated that this mode can be successfully used as an infrared probe of the several transitions which occur in this section of the phase diagram, being very sensitive to the crystal structure as well as to site rearrangements. We found that the *A* and *B* room-temperature phases are stable to about 90 K. Below this temperature and 8–9 GPa exist the crsytal modifications observed at 4 K in Raman[6,13,15] and, partially, in NMR (Ref. 16) experiments. Boundaries of all these phases have been accurately drawn and, taking advantage of lower temperature experiments, extrapolated down to 0 K. A different phase has been observed over 25 GPa at room temperature. The transition to this phase has been studied isothermally at several different temperatures. The results show that this is a stable methane crystalline modification from 300 down to 0 K.

Group-theoretical arguments suggest for the single-site HP phase four different unit-cell symmetries: D_{4h}, D_{6h}, T_h, O_h. Qualitative close-packing considerations and similarities with rare gases[25–27] and ammonia,[28,29,30] for which the hexagonal structure is likely stabilized by anisotrophic interactions, favor the D_{6h} factor group with molecules on C_s sites.

The symmetry considerations, combined to the present information on the phase diagram and to the kinetics of the different phase transitions, allow us to sketch a detailed structural analysis of the different phases. The *A*-*B* and IV-V transitions appear extremely difficult to occur, while all others take place easily and reversibly either in compression or expansion experiments. On this basis and taking into account the evolution of the fcc-hcp transitions observed either experimentally[25] or theoretically,[24] it may be said that methane crystal evolves from a fcc (I and II) to a close-packed hcp single-site structure (HP) through intermediate multisite tetragonal (III, IV, and maybe *A*) and hexagonal (V, VI, and *B*) modifications. Considering also Raman results and assuming valid the three-site model for phases III, IV, V, and VI, we propose a consistent evolution of the site symmetry. A direct characterization of the high-pressure phases is still certainly needed and one of the aims of this work is to stimulate x-ray diffraction studies.

ACKNOWLEDGMENTS

This work was supported by contract with European Community (GE1*CT92-0046) and by the Italian Ministero Universita' e Ricerca Scientifica e Tecnologica (MURST). A special acknowledgment is due to Professor P. R. Salvi for the critical reading of the manuscript and for important suggestions.

*Permanent address: Laboratorio di Spettroscopia Molecolare, Dipartimento di Chimica, Universita' di Firenze, Via G. Capponi 9, 50121 Firenze, Italy.

†Present address: ILL-Institut Laue-Langevin, Boîte Postale 156, 38042 Grenoble Cédex 9, France.

[1] D. P. Cruikshank, T. L. Roush, T. C. Owen, T. R. Geballe, C. De Bergh, B. Schmitt, R. H. Brown, and M. J. Bartolomew, Science **261**, 742 (1993).

[2] T. C. Owen, T. L. Roush, D. P. Cruikshank, D. P. Elliot, J. L. Young, C. De Bergh, B. Schmitt, T. R. Geballe, R. H. Brown, and M. J. Bartolomew, Science **261**, 745 (1993).

[3] E. Quirico, B. Schmitt, R. Bini, and P. R. Salvi, Planet. Space Sci. **44**, 973 (1996).

[4] M. S. Somayazulu, L. W. Finger, R. J. Hemley, and H. K. Mao, Science **271**, 1400 (1996).

[5] W. Press, J. Chem. Phys. **56**, 2597 (1972).

[6] D. Fabre, M. M. Thiery, H. Vu, and K. Kobashi, J. Chem. Phys. **71**, 3081 (1979).

[7] F. D. Medina and W. B. Daniels, J. Chem. Phys. **70**, 2688 (1979).

[8] B. W. Baran and F. D. Medina, Chem. Phys. Lett. **176**, 509 (1991).

[9] P. Calvani and S. Lupi, J. Chem. Phys. **90**, 5294 (1989).

[10] M. Praeger, W. Press, and A. Heidemann, J. Chem. Phys. **72**, 5294 (1980).

[11] M. Praeger, W. Press, A. Heidemann, and C. Vettier J. Chem. Phys. **77**, 2577 (1982).

[12] A. I. Prokhvatilov and A. P. Isakina, Acta Crystallogr. B **36**, 1576 (1980).

[13] D. Fabre, M. M. Thiery, and K. Kobashi, J. Chem. Phys. **76**, 4817 (1982).

[14] F. D. Medina, Chem. Phys. Lett. **85**, 91 (1982).

[15] D. Fabre, M. M. Thiery, and K. Kobashi, J. Chem. Phys. **83**, 6165 (1985).

[16] D. Van der Putten, K. O. Prins, and N. J. Trappeniers, Physica B **114**, 281 (1982).

[17] P. Hebert, A. Polian, P. Loubeyre, and R. Le Toullec, Phys. Rev. B **36**, 9196 (1987).
[18] R. Bini, L. Ulivi, H. J. Jodl, and P. R. Salvi, J. Chem. Phys. **103**, 1353 (1995).
[19] R. Ballerini, R. Bini, G. Pratesi, and H. J. Jodl, Rev. Sci. Instrum. (to be published).
[20] K. H. Mao, P. M. Bell, J. W. Shaner, and D. J. Steinberg, J. Appl. Phys. **49**, 3276 (1978).
[21] S. Califano, V. Schettino, and N. Neto, *Lattice Dynamics of Molecular Crystals*, Lecture notes in Chemistry Vol. 26 (Springer, Berlin, 1981).
[22] S. Califano and V. Schettino, Int. Rev. Phys. Chem. **7**, 19 (1988).
[23] K. Maki, Y. Kataoka, and T. Yamamoto, J. Chem. Phys. **70**, 2688 (1979).
[24] M. Parrinello and A. Rahman, J. Appl. Phys. **52**, 7182 (1981).
[25] A. P. Jephcoat, K. H. Mao, L. W. Finger, D. E. Cox, R. J. Hemley, and C. Zha, Phys. Rev. Lett. **59**, 2670 (1987).
[26] M. Grimsditch, P. Loubeyre, and A. Polian, Phys. Rev. B **33**, 7182 (1986).
[27] A. Polian, J. M. Besson, M. Grimsditch, and W. A. Grosshans, Phys. Rev. B **39**, 1332 (1989).
[28] J. W. Otto, R. F. Porter, and A. L. Ruoff, J. Phys. Chem. Solids **50**, 171 (1989).
[29] S. Klotz, M. Gauthier, J. M. Besson, G. Hamel, R. J. Nelmes, J. S. Loveday, R. M. Wilson, and W. G. Marshall, Appl. Phys. Lett. **67**, 1188 (1995).
[30] J. S. Loveday, R. J. Nelmes, W. G. Marshall, J. M. Besson, S. Klotz, and G. Hamel, Phys. Rev. Lett. **76**, 74 (1996).
[31] T. Yamamoto, Y. Kataoka, and K. Okada, J. Chem. Phys. **66**, 2701 (1977).
[32] K. J. Lushington, K. Maki, J. A. Morrison, A. Heidemann, and W. Press, J. Chem. Phys. **75**, 1410 (1981).